Growth Cone Localization of Neural Cell Adhesion Molecule on Central Nervous System Neurons In Vitro

Anthony N. van den Pol,* Umberto di Porzio,*‡ and Urs Rutishauser§

*Section of Neurosurgery, Yale University School of Medicine, New Haven, Connecticut 06510; ‡Institute of Molecular Embryology, Consiglio Nazionale delle Ricerche, Arcofelice, Naples, Italy; and §Department of Developmental Genetics and Anatomy, Case Western Reserve University School of Medicine, Cleveland, Ohio 44106

Abstract. Ultrastructural analysis of colloidal gold immunocytochemical staining and immunofluorescence microscopy has been used to study the presence of neural cell adhesion molecule (NCAM) on the surface of neuronal growth cones. The studies were carried out with cultures of rat hypothalamic and ventral mesencephalic cells, using morphology and expression of tyrosine hydroxylase, neurofilaments, and glial fibrillary acidic protein as differential markers for neurons and glia. NCAM was found on all plasmalemmal surfaces of neurons including perikarya and neurites. The density of NCAM varied for different neurons growing in the same culture dish, and neurons had at least 25 times more colloidal gold particles on their plasmalemmal membranes than astroglia. Of particular interest in the present study was a strong labeling for NCAM on all parts of neuritic growth cones, including the lamellar and filopodial processes that extend from the tip of the axon. The density of NCAM was similar on different filopodia of the same growth cone. Therefore, in situations where homophilic (NCAM–NCAM) binding might contribute to axon pathfinding, a choice in direction is more likely to reflect differences in the NCAM content of the environment, rather than the distribution of NCAM within a growth cone. On the other hand, the variation in NCAM levels between single neurons in culture was significant and could provide a basis for selective responses of growing neurites.

DURING development of the central nervous system (CNS),[1] axons can travel considerable distances to synapse with specific target neurons. The question of what cues are used by the growing axon to traverse a complex cellular environment to reach the appropriate target is critical to understanding the generation of neuronal connections. A number of factors, including physical channels and barriers, preestablished paths, glial guidance, and electrical fields (2, 6, 19, 31, 35, 36, 46, 55) have been postulated as contributing to the guidance of axons. Chemotactic cues may also play a role in axonal guidance, and may involve either a gradient distribution of diffusible factors such as nerve growth factor (28) or distribution of membrane or substrate-bound molecules involved in cell recognition and adhesion (26, 44, 47, 49). With respect to cell–cell adhesion, spatial and temporal differences in the amount and form of the neural cell adhesion molecule (NCAM) may also serve to provide cues for axon pathfinding and target recognition (11, 20, 30, 45, 48).

NCAM is an integral cell surface glycoprotein directly involved in the formation of bonds between cells that express it on their surface (11, 13, 38, 43). Binding mediated by NCAM appears to involve a homophilic interaction between NCAMs on different cells (42), and the molecule has been identified on the surface of neurons (40, 43), muscle cells (14, 41), and glia (23, 25, 29). Accordingly, NCAM-mediated adhesion has been found to participate in the fasciculation of neurites in culture (40), retinal ganglion cells in the optic nerve (38), the formation of a stable association between axons and myotubes (41), and the interaction of pioneer retinal fibers with the endfoot region of glial cell precursors (45).

Growth cones, particularly their filopodia and lamellipodia, are believed to play a key role in axonal guidance during vertebrate neural development (1, 2, 17, 27). In studies on the function of NCAM-mediated adhesion in axon pathfinding, it has generally been assumed that the adhesion involves the nerve growth cone. However, the presence of NCAM on this structure has only been inferred from observations at the level of light microscopy (39). To determine the distribution of NCAM on the growth cone, including lamellipodia and filopodia, we have analyzed neurons in a monolayer tissue culture model system (7, 8) allowing both a gross localization by immunofluorescence light microscopy, and a quantitative evaluation by colloidal gold immunocytochemistry and elec-

1. *Abbreviations used in this paper:* CNS, central nervous system; GFA, glial fibrillary acidic protein; NCAM, neural cell adhesion molecule; TH, tyrosine hydroxylase.

tron microscopy (50). Together, these methods have been used to evaluate the relative number of NCAM molecules on the surfaces of different cells. A preliminary report of some of our data has appeared previously (52).

Methods

Tissue Culture

Mesencephalic and hypothalamic cell cultures were prepared using Sprague Dawley rat (Charles River Breeding Laboratories, Inc., Wilmington, MA) embryos of day E12 to E15, and E16 to E18, respectively. Brains were removed and placed in sterile phosphate-buffered saline (PBS) supplemented with 6 mg/ml glucose, and the two regions of interest transferred to a dish containing plating medium. Cells were dissociated by repeated passage through a Pasteur pipette (34). Proteolytic enzymes such as trypsin were not used as they might cleave the NCAM molecule from the membrane. After dissociation, cells were pelleted by centrifugation, and resuspended to 500,000/ml in Dulbecco's minimum essential medium (Gibco, Grand Island, NY), supplemented with 2 mM glutamine, 4.5 mg/ml glucose, 8% heat-inactivated fetal calf serum (Gibco), and 8% heat-inactivated horse serum (Gibco). 1 ml of cell-suspension was plated on 6-well 35-mm plates (Costar, Data Packaging Corp., Cambridge, MA) that were previously coated with an aqueous solution of 4 μg/ml polyornithine (40,000 mol wt; Sigma Chemical Co., St. Louis, MO) for 1 h at 37°C and washed three times in sterile water. Cultures were kept in 5% CO_2 at 37°C in 100% humidity in an incubator (model 6100, Napco Industries, Inc., Hopkins, MN). The tissue culture medium was changed once a week. Neurons survived in these cultures for more than 3 wk.

The cultures derived from the hypothalamus and mesencephalon contained both neuronal and glial cells. As controls for staining specificity we also cultured human fibroblasts and primary fibroblasts from E16 rat hind limb epidermis. The fibroblast cultures were used after three passages from successive confluent cultures. To obtain a more homogeneous glial culture as a further control for NCAM immunostaining, 10–20-d-old cultures were treated with trypsin (0.2% in PBS for 5 min at 37°C); proteolysis was stopped by the addition of serum to final concentration of 10%. Cells were resuspended, dissociated with passage through a Pasteur pipette, centrifuged, and replated at low concentrations (200,000/dish) on polyornithine-treated culture dishes, and allowed to grow for at least 4 d before use.

NCAM Antiserum

The NCAM antigen was obtained by immunoaffinity chromatography from a Nonidet P-40 detergent extract of brain membrane vesicles from 4-wk-old BALB/c mice. The purified NCAM migrated in SDS polyacrylamide gel electrophoresis as a group of diffuse bands characteristic of the carbohydrate-containing molecule as previously reported (11, 37).

Rabbit antisera to NCAM were prepared by injection of 100 μg antigen in complete Freund's adjuvant followed by three monthly boosts of 20 μg antigen in incomplete Freund's adjuvant. 7 d after the last injection, serum was obtained. Immunoblots (16) of SDS gel electrophoresis-fractionated 4-wk mouse brain extract resulted in the staining of prominent bands of apparent mol wt 180,000, 140,000, and 120,000, characteristic of total NCAM from this tissue (11, 37). The antiserum also recognized the NCAM molecule after removal of sialic acid. Comparison of this antiserum with anti-BSP-2 and anti-D2-CAM (names for NCAM used by other laboratories) indicated that all three reagents recognized the same three polypeptides. Furthermore, immunoreactivity using the same antiserum used in the present studies can be eliminated by preabsorption of the NCAM antigen with either BSP-2 or D2-CAM antisera (29). Additional characterization of the NCAM antiserum is described elsewhere (29).

Fixation and Immunocytochemistry

A fixation that allowed both antigen recognition and adequate ultrastructural preservation consisted of a 15–60-min treatment with 4% freshly depolymerized paraformaldehyde with 0.05% glutaraldehyde in 0.1 M phosphate buffer, pH 7.4. Longer periods of fixation inhibited specific staining, as did higher concentrations of glutaraldehyde. After fixation, cultures were rinsed (3 × 5 min) in buffer, and then incubated for 15 min in a blocking solution consisting of 5% normal goat serum, 1% bovine serum albumin (BSA), and 0.1% glycine in PBS.

For immunofluorescence staining, the cells were exposed for 20–40 min to rabbit antiserum against NCAM at a dilution ranging from 1:70 to 1:250. After three rinses in buffer, cultures were incubated with goat anti-rabbit IgG conjugated to fluorescein isothiocyanate (EY Labs, San Mateo, CA) at a dilution of 1:100 to 1:250, washed, and examined with an Olympus fluorescence microscope. Staining of live cells was performed in the same way, except cells were fixed after immunostaining. For immunogold staining, an affinity-purified goat anti-rabbit IgG adsorbed to 10-nm colloidal gold was used (5, 21, 50, 51) at a concentration that gave a submaximal level of gold particle labeling; this low level of staining was necessary to minimize lateral steric hinderance that would hinder quantitative analysis.

As a control for staining specificity, 10 μg of purified mouse NCAM antigen was mixed with 1 ml of the antiserum at a 1:140 dilution for 4 h at room temperature with constant agitation. Preincubation of the NCAM antiserum with purified mouse NCAM blocked NCAM immunostaining as visualized by either fluorescence microscopy or ultrastructural colloidal gold immunocytochemistry. Substitution of normal rabbit serum for the NCAM antiserum resulted in no specific staining.

To verify the neuronal or glial origin of some processes in vitro, we used antisera against the dopamine rate-limiting synthesizing enzyme tyrosine hydroxylase (TH) (53) (gift of Dr. J. Powell, Oxford University, Oxford, England) which is found only in catecholaminergic neurons and not in glial cells, against 200,000-kD neurofilaments (Labsystem, Finland), and against glial fibrillary acidic protein (GFA) (gift of Dr. L. Eng, Stanford, University, Stanford, CA). The number of dopaminergic neurons in these rat cultures, similar to cultures of mouse embryonic mesencephalon (34), is very low (<1%). Therefore, the use of TH-antiserum also enabled us to follow a cell from its soma to the tip of growing neurites. Antiserum against TH or GFA gave no staining unless the plasmalemmal membrane was permeabilized first with detergent or by freeze-thawing. Neither freeze-thawing nor detergent (0.5% Triton X-100 for 30 min) treatment reduced NCAM immunofluorescence.

Under the conditions of our experiments, neurons and glial cells can generally be recognized by light microscopy according to their different shapes. To allow a better differentiation of these cells when studied by electron microscopy, we used a multiple-staining procedure for NCAM and TH. After staining for NCAM with immunogold as described above, cells were permeabilized by freeze-thawing, incubated with TH antiserum, then stained (both extracellularly for NCAM and intracellularly for TH) with avidin-biotin-peroxidase reagents obtained from Vector Laboratories, Inc. (Burlingame, CA) (54). After immunostaining, cultures were postfixed in 1% osmium tetroxide for 10 min, quickly dehydrated, and embedded in an Epon mixture consisting of 17.2 ml dodecenyl succinic anhydride, 24.4 ml Epon 812, 8.5 ml nadic methyl anhydride, and 1 ml 2,4,6tri(dimethyl aminomethyl)phenol. After removal of the Epon block from the culture dish, small blocks were prepared with an orientation either parallel or perpendicular to the surface of the culture dish. Thin silver sections were picked up on 300-mesh or Formvar-coated single slot grids, and lightly stained with uranyl acetate and lead citrate.

Colloidal Gold Quantitation

Photomicrographs (52,000×) were placed on a digitizer (Bit Pad, Summagraphics Corp., Fairfield, CT) interfaced with a microprocessor (North Star Computers, Inc., San Leandro, CA). The curvilinear lengths of membranes directly exposed to tissue culture medium were measured, and the number of colloidal

Figure 1. Staining of cultures with antibodies against GFA, TH, neurofilaments, and NCAM. (*A*) Photomicrograph of cultured cells by Nomarski optics after 7 d in culture. Both neurons (*N*) and astroglia (*AS*) can be seen. A number of neuritic processes (*P*) are found both over flat astrocytes and over the polyornithine-treated plastic. Bar, 43 μm. (*B*) Neuron immunoreactive for TH with growth cone (*arrow*, 5 μm) from a thick process. (*C*) Arrow (10 μm) indicates growth cone at the terminal end of a long thin neuritic process immunoreactive for TH. (*D*) Fluorescence microscopy of glial cells stained with antiserum against GFA. Bar, 10 μm. (*E*) Neuronal processes and cell bodies stained with antiserum to NCAM and lying for the most part over unstained astrocytes. Bar, 20 μm. (*F*) Neurons immunoreactive for neurofilaments. Bar, 20 μm. E18 hypothalamus after 4 (*B* and *C*) and 7 (*A*, *D*, *E*, and *F*) d in vitro.

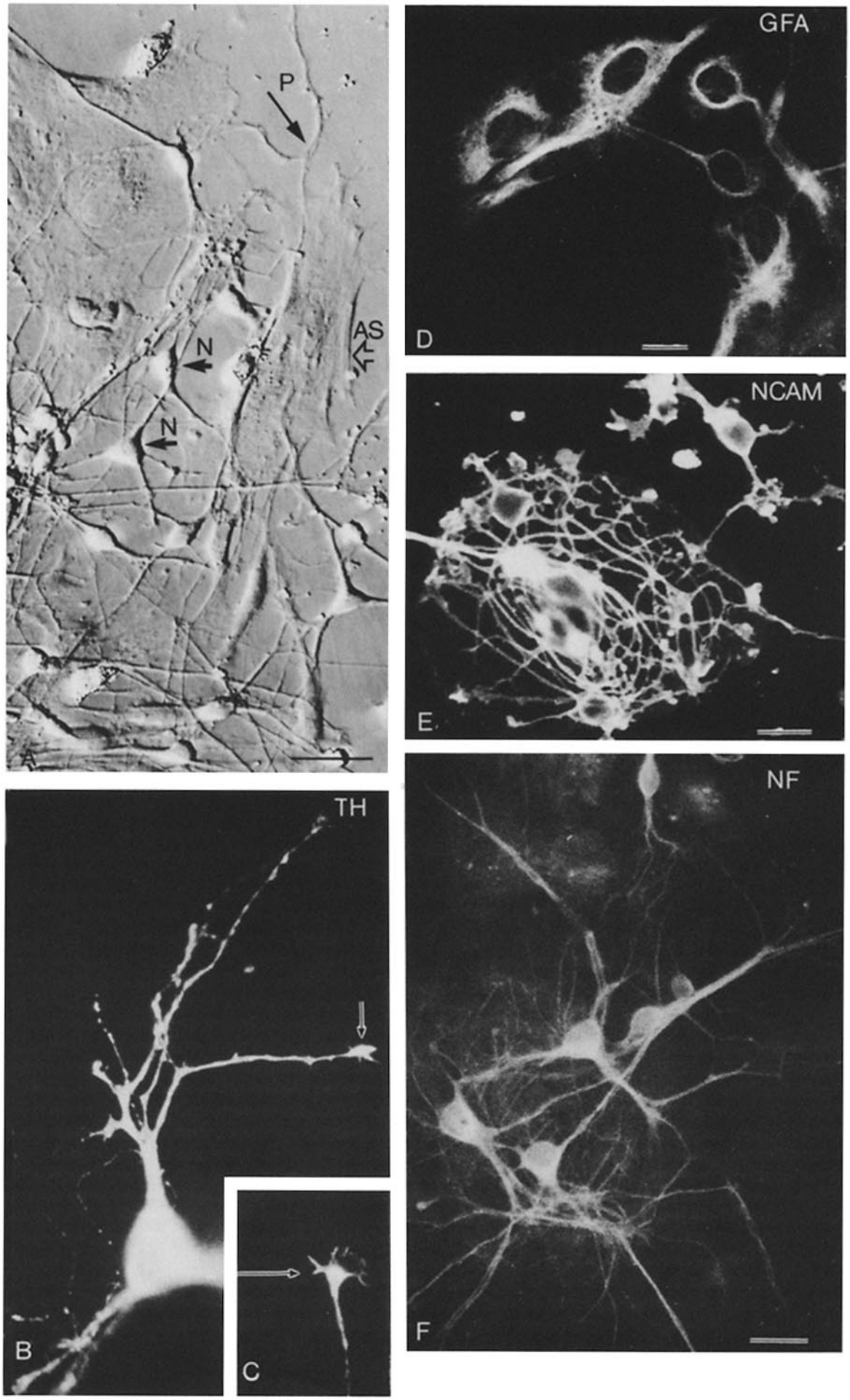
P
AS
N
N
A
TH
B
C
GFA
D
NCAM
E
NF
F

gold particles labeling that membrane was counted. Since colloidal gold can aggregate, two or more aggregated particles with no space between them were counted as a single unit. Membranes with overlying structures were excluded from this analysis. To compare the relative densities of colloidal gold on different neurons in the same culture well, the number of gold particles per micrometer was counted on different membrane regions near the perikaryon.

Results

Identification of Cells and Growth Cones in Monolayer Cultures

After disaggregation and plating of embryonic hypothalamus and mesencephalon, all of the cells initially had a round morphology. Within a few hours of culture, neuritic extension was observed from some cells. Within 1 d, all cells had undergone considerable differentiation. Glial cells began to flatten, and neuronal processes were found arising from most neurons. Within 2 d neuronal processes grew over both the polyornithine-coated plastic substrates and over flattened glial cells (Fig. 1*A*).

To verify the morphological identification of glial cells, an antiserum to GFA, which is found in astrocytes but not in neurons, was used. Most GFA-stained cells were large and flat, with GFA filaments radiating out from the cell body (Fig. 1*D*). A second type of cell staining with GFA had a few large processes which extended from the cell body no more than 100 μm. These processes were thicker than neurites, and could also be distinguished ultrastructurally from neurites by their bundles of glial filaments and characteristic membrane specializations.

Dopaminergic neurons are particularly concentrated in the rostral ventral mesencephalon and hypothalamus (53). To facilitate delineation of morphological characteristics of neurons, we examined dopaminergic cells stained immunocytochemically with an antiserum against TH (Fig. 1, *B* and *C*). TH immunoreactive neurons had a phase-bright perikaryon, and from two to four thin processes arising from the cell body. In younger cultures the processes from a single cell appeared similar in morphology; axons and dendrites could not be differentiated. After 7 d in vitro, one process could often be identified as a putative axon; this process was generally quite long with a constant diameter, branched frequently, and had a total length of up to several millimeters. In contradistinction, two or three other processes could be identified as putative dendrites, tapering from proximal to distal, and branching infrequently. Cells stained with neurofilament antiserum (Fig. 1*F*) had a similar morphology to cells stained with TH antiserum; as expected, more cells were immunoreactive for neurofilaments than for TH. Growth cones were more clearly seen with TH antiserum (Fig. 1*C*) than with neurofilament antiserum (Fig. 1*F*). Flat phase-dim cells were not immunoreactive with TH or neurofilament antisera.

In our cultures, CNS neuron growth cones, identified by morphology or TH-staining, had the same general characteristics as those found at the growing tips of cultured neurons of the peripheral nervous system (1, 3). Single neuritic growth cones had an overall morphology similar to a flattened hand, with a flat area at the distal end and thin lamellipodia and filopodia radiating out from the lateral perimeter. Filopodia were sometimes fairly thick proximally, thinning down distally to ~0.1 μm in diameter, below the resolution of light microscopy. The track taken by the growth cone is revealed by the shape of the neurite. In our cultures neurites seldom grew in straight lines, but generally showed a curvilinear growth pattern; this was evident on the polyornithine coated plastic, and particularly evident on underlying astroglia (Fig. 1*E*).

When examined ultrastructurally CNS growth cones had the same complement of organelles described previously for peripheral neurons. What appeared by light microscopy to be a single growth cone often was revealed by electron microscopy to be composed of several neurites growing together. At the distal end of such a fascicle, either a single or several flattened growth cones could be located. Growth cones located along other neurite shafts had a more compact "torpedo-like" appearance.

NCAM Distribution by Immunofluorescence Microscopy

An intense fluorescence immunostaining for NCAM was seen on neuron cell bodies and their processes, including both the neurite and growth cone (Fig. 1*E*, 2). Strong staining for NCAM appeared to be restricted to cells with a neuronal shape, similar in morphology to cells stained for TH or neurofilaments, and dissimilar from cells immunoreactive for GFA (Fig. 1). No obvious differences in intensity were seen with fluorescence staining on different parts of the same cell.

Labeling around the external tip of the growth cone and along that part of the proximal filopodia which could be seen by fluorescence microscopy consistently appeared more intense than on the flat astrocytes used for comparison in the same culture dish. Similar to growth cones stained with TH, NCAM immunoreactive filopodial extensions radiated out from the edges of growth cones with an occasional bifurcation of small filopodial extensions. NCAM-positive filopodial processes were found reaching across the plastic substrate to contact other growth cones, neurites, or even the trailing neurite of the parent growth cone (Fig. 2*C*). That neurons and all parts of their growth cones were brightly immunofluorescent in contrast to the dim staining of flat astrocytes was confirmed with NCAM antisera from two additional sources (gifts of Dr. O. S. Jorgensen, Rigshospitalet, Copenhagen, and J. Sanes and J. Covault, Washington University, St. Louis, MO).

Using the same antibody dilutions which resulted in positive neuronal staining for NCAM, no fluorescence staining was seen either on human or rat fibroblasts after 1 wk in vitro. Relative to the bright staining of neurons, the faint fluorescence observed on flat glial cells was more evident with higher concentrations of antisera, and was only slightly stronger than the presumed background labeling found on fibroblasts cultured in the absence of neurons. Glial cultures grown in the virtual absence of neurons for 4 d also showed only a slight immunofluorescence with NCAM antisera, but strong immunostaining with GFA antiserum.

NCAM Distribution by Immunogold Electron Microscopy

With electron microscopy and colloidal gold immunostaining, NCAM was found over all parts of neuron-like cells, including

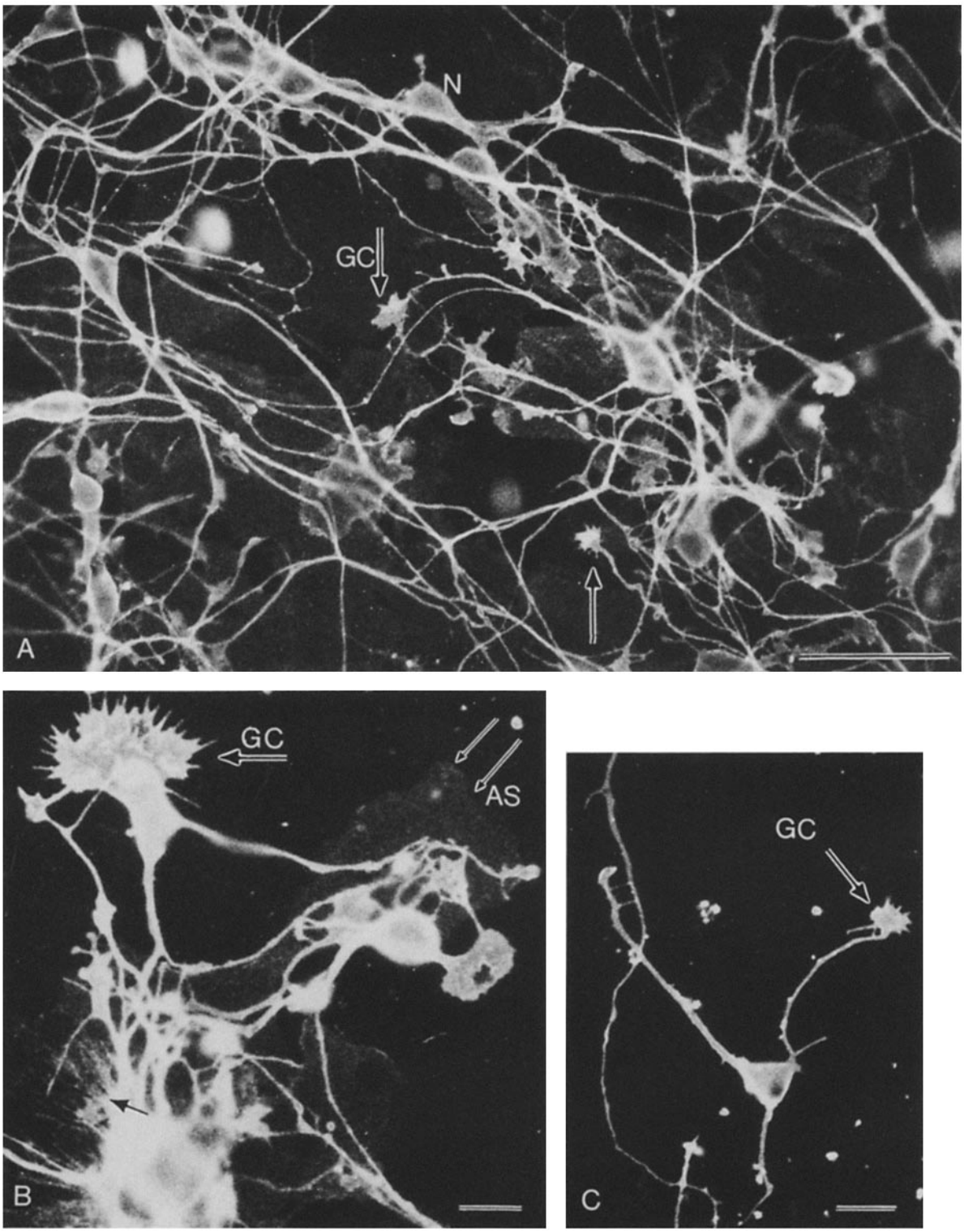

Figure 2. NCAM immunofluorescence staining of cells, neuritic processes, and growth cones. (*A*) Both neuronal perikarya (*N*) and processes are strongly stained with NCAM. Growth cones (*arrows*) of several different shapes can be found throughout the neuropil. (*B*) A particularly large growth cone (*GC*) is seen with lamellipodia and filopodial extensions. Such a large growth cone may actually be made up of several growth cones from different cells growing in the same place, as confirmed by ultrastructural analysis. A large number of thin filopodial extensions reach out from a group of several NCAM immunoreactive cells (*black arrow*), possibly representing filopodial extensions from a number of growth cones growing in the regions of the somata. (*C*) Filopodial extension from growth cone reaches back to contact neurite of origin. E13 mesencephalon after 7 d in culture. Bars: (*A*) 35 μm; (*B*) 15 μm; (*C*) 15 μm.

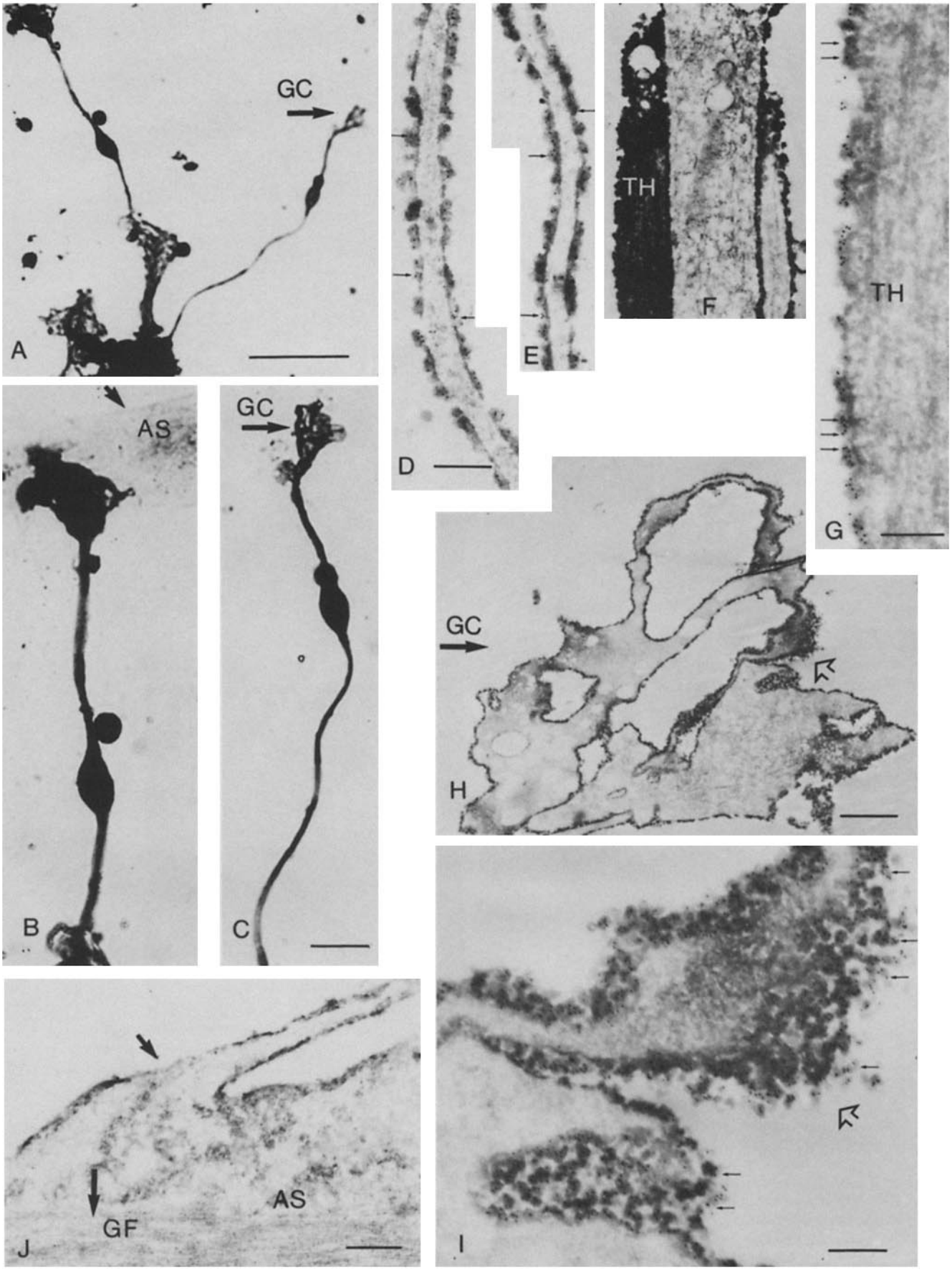
GC
A
AS
B
GC
C
D
E
TH
F
TH
G
GC
H
I
AS
GF
J

the cell body, neurites, and growth cones. The labeling density of gold particles was much greater on neurons than on adjacent flat glial cells. To confirm the association of the immunogold staining with neurons, cultures were stained for NCAM by both the colloidal gold and immunoperoxidase methods, and then for cytoplasmic TH using peroxidase (Fig. 3). All neurons appeared to have both gold and peroxidase labeling for NCAM (Fig. 3, *D–I*). A subpopulation of these neurons had cytoplasmic peroxidase staining indicating the presence of TH. Unlike neuronal filopodia, filopodial extensions from glia showed no evidence of immunogold NCAM or peroxidase TH immunolabeling (Fig. 3*J*).

To facilitate a direct comparison of colloidal gold labeling of neurons, glia, and their processes, several micrographs (Figs. 4–7) were taken from a single culture plate. These cells were cut in thin sections perpendicular to the culture plate. Fig. 4*A* shows a neuron cell body with strong gold labeling over the plasmalemma; the density of gold labeling on this cell can be compared with the cell body of the flat astrocyte (Fig. 4*B*) with only a sparse labeling by gold particles, similar to glial processes (Fig. 4*C*) which also showed negligible gold labeling. Neurons growing on top of flat glia (Fig. 5*A*) consistently displayed a higher level of gold labeling than the exposed plasmalemma of the underlying glial cell. A phase-bright nonneuronal cell contacted by an adjacent cell through a membrane specialization, and showing microvilli-like protuberances from the perikaryon, had no gold label on it (Fig. 5*B*).

When examined in cross-section, neurites growing over glial cells were labeled with gold (Fig. 6). The absence of neuronal staining at points of neurite–neurite (Fig. 6*B*) and neurite–astrocyte (Fig. 6*C*) contact probably reflects poor penetration of immunocytochemical reagents rather than the absence of NCAM. Glial cells, however, did not stain either in regions of cell–cell contact or in areas of exposed membrane. Serial thin sections through some regions revealed processes with the appearance of neuronal filopodia during a retraction phase during which the filopodia were not pulled straight out from the tip of the growth cone; alternatively, during the process of fixation and embedding, filopodia may have become dislodged from sites of their normal adhesion. These processes were heavily labeled with gold (Fig. 7*A*) as were terminal processes with large numbers of clear vesicles suggestive of terminal growth cones (Fig. 7*B*). Similarly, in sections cut parallel to the bottom of the culture dish (Fig. 8), gold particles were found labeling thin finger-like extensions from growth cones.

Quantitative Evaluation of NCAM Labeling

Neurons averaged 12.4 gold particles/μm membrane length, while glia showed 0.5 particles/similar length. This difference was significant at the $P < 0.001$ level ($t = 15$, $df = 40$). To compare the density of colloidal gold NCAM immunolabeling on different neurons under identical experimental conditions, the number of gold particles per each micrometer of membrane was counted from hypothalamic cells within a 200 μm radius of one another. From measurements of 8–10 membrane areas/cell, the means and SDs of NCAM immunogold labeling for each of eight neurons examined were 6.4 ± 2.1, 14.2 ± 2.2, 6.6 ± 1.7, 14.3 ± 5.1, 8.9 ± 2.3, 15.4 ± 1.3, and 7.3 ± 1.9. Based on an analysis of variance of the combined data, the difference in the density of gold particle labeling on different neurons was highly statistically significant ($F = 55.3$, $df = 5/65$, $P < 0.0001$), indicating a marked heterogeneity in cellular expression of NCAM with over a twofold difference between neurons.

Discussion

During axonal growth, long thin filopodia extend from the growth cone. If some of them stick to a particular surface, the orientation of the entire growth cone can be shifted in the direction of that adhesion (2). When filopodia from the same growth cone contact several different surfaces, the direction of growth is toward the most adhesive one (27). In the present study we demonstrate that NCAM is present in high densities on filopodial processes. Therefore, if another neurite or cell body with NCAM on its surface is contacted by these filopodia, the resulting homophilic adhesion could influence the path of subsequent growth. A choice of directions could then be dictated, in the absence of other more dominant influences, by either a difference in the density of NCAM among different filopodia of a single growth cone, or a difference in the amount of NCAM on different cells that comprise the surrounding environment.

Although the density of NCAM differed from cell to cell in the present study, the distribution over a single cell was quite

Figure 3. Simultaneous staining for NCAM and TH, as viewed by light (*A–C*) and electron (*D–I*) microscopy. To correlate the general morphology of cells with immunogold ultrastructural analysis for NCAM distribution, neurons were also stained for membrane-associated NCAM and cytoplasmic TH using peroxidase immunohistochemical procedures. (*A*) At the bottom of the micrograph is a small group of cells. Two bipolar neurons are associated with fascicles that extend down to the group of cells, and up to end in a group of growth cones (*GC*) (*arrow*). Bar, 60 μm. All other parts of this figure are taken from different regions of the cells shown in *A*. (*B*) One bipolar cell with processes extending up to an underlying unlabeled astrocyte (*AS*). (*C*) The second bipolar cell with growth cones directly in contact with the substratum. Bar (*B* and *C*), 15 μm. (*D* and *E*) Thin filopodial extensions from the growth cone in *C*, showing both peroxidase and immunogold labeling (*arrows*) for NCAM. Bar, 280 nm. (*F*) Cytoplasmic labeling for TH of one neurite; two other neurites have unlabeled cytoplasm. This fascicle belongs to the process extending downward in *C*. All three neurites have peroxidase labeling for NCAM on the cell surface; in this photograph immunogold particles are obscured by the dense stain. Bar, 0.58 μm. (*G*) Higher magnification of the TH-positive process from *F* with photographic exposure that enables visualization of colloidal gold labeling for NCAM. Bar, 0.15 μm. (*H*) Growth cone found at arrow with peroxidase labeling for NCAM at low magnification. Bar, 1 μm. (*I*) Same growth cone at higher magnification (bar, 0.2 μm), showing both peroxidase and immunogold labeling for NCAM. (*J*) Part of an astrocytic filopodium extending from the astrocyte seen by light microscopy in *B*. Note the lack of colloidal gold labeling in contrast to the neuronal filopodia. (*AS*, astrocyte; *GF*, glial filaments). Bar, 0.28 μm. E13 mesencephalon after 3 d in vitro.

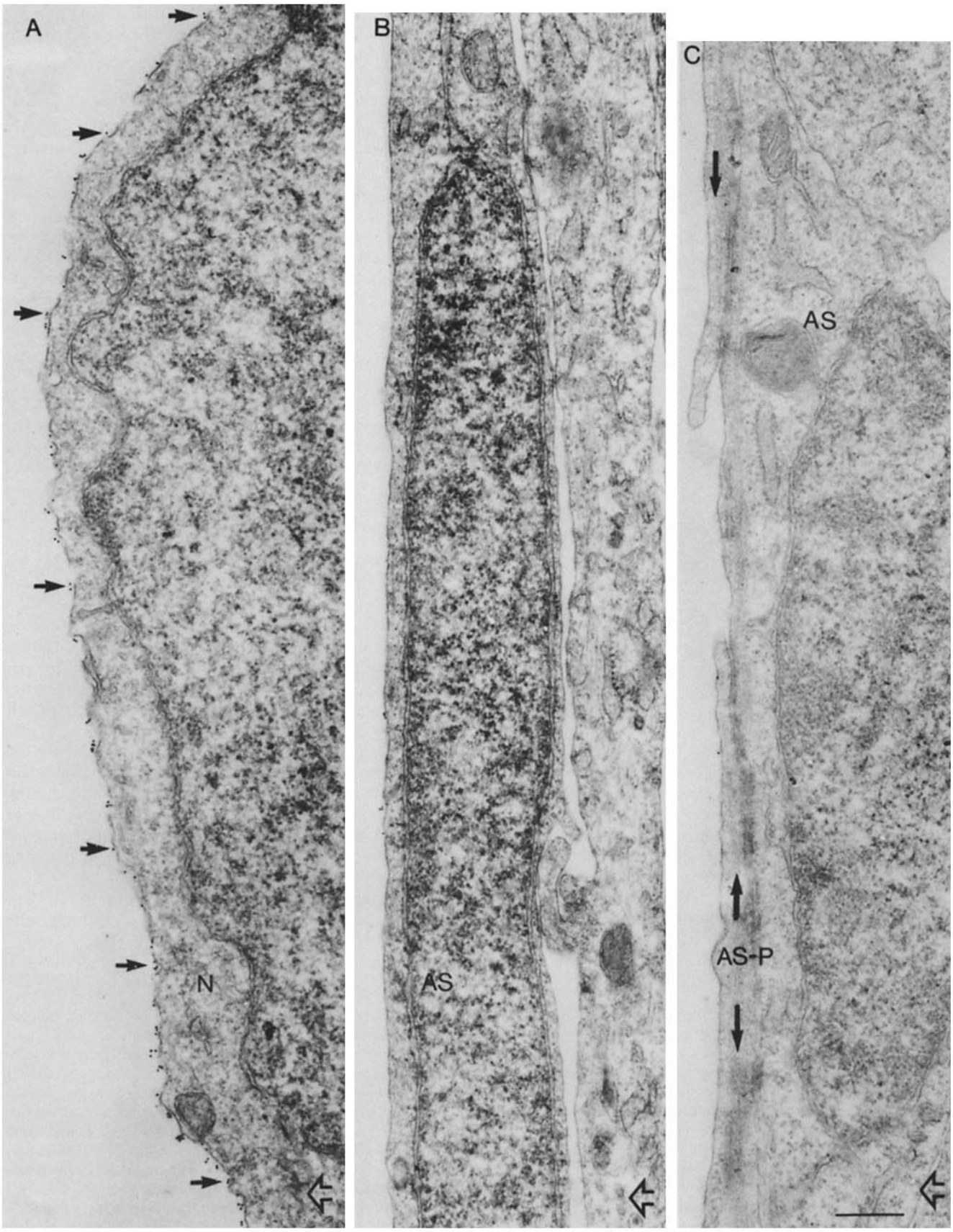

Figure 4. Immunogold staining for NCAM. (*A*) Labeling of NCAM on neuronal perikaryal (*N*) plasmalemma. (*B*) Astrocyte (*AS*) soma shows little labeling for NCAM. Most astrocyte cell bodies were flat, not extending more than 3 μm high above the bottom of the culture plate. Astrocytic nuclei were often not over 1 μm high, but extended ≥10 μm in diameter. Here an astrocyte soma is shown growing over another astrocyte. (*C*) Similarly, astrocytic processes (*AS-P*) show little gold labeling. Hollow arrows indicate which direction is up from the bottom of the culture dish. Sections were cut perpendicular to the bottom of the culture dish. E18 hypothalamus after 4 d in vitro. Bar, 0.39 μm.

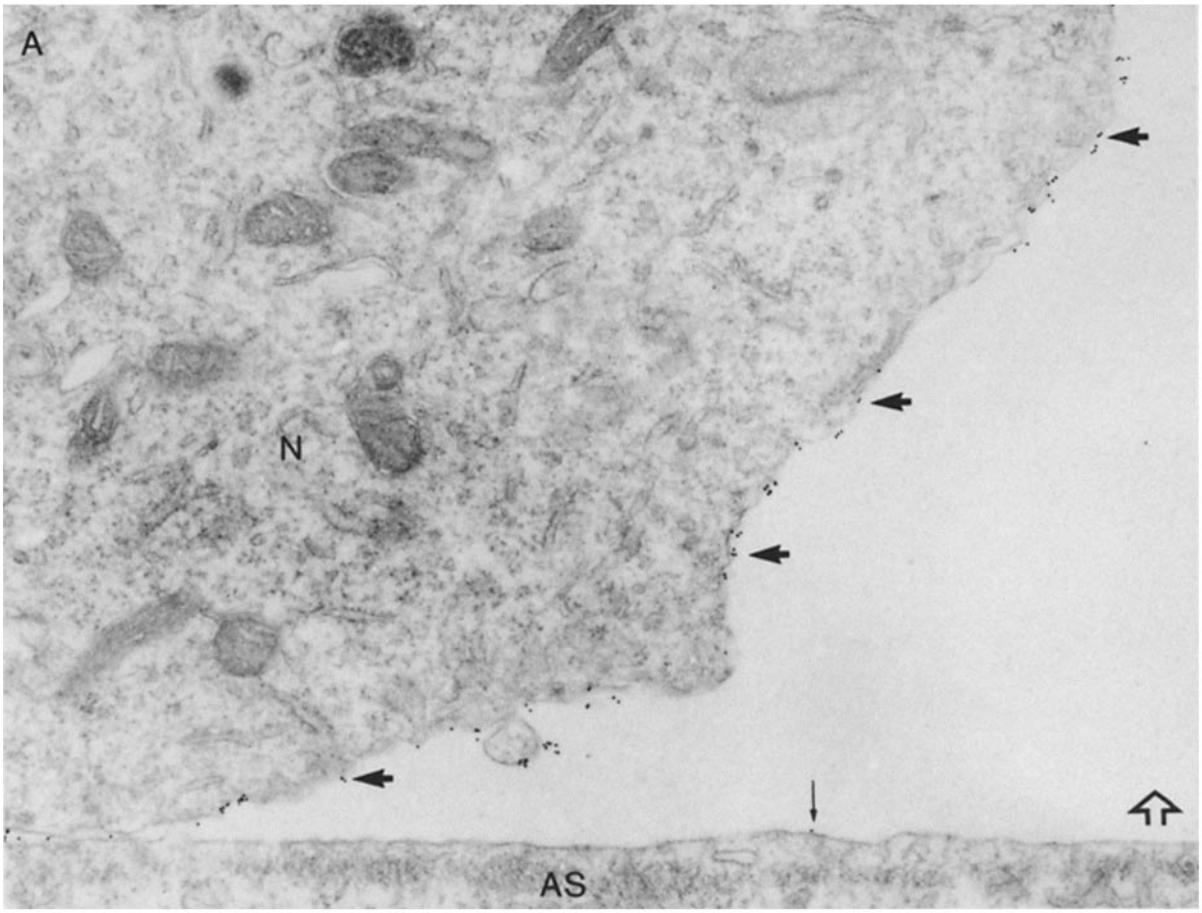

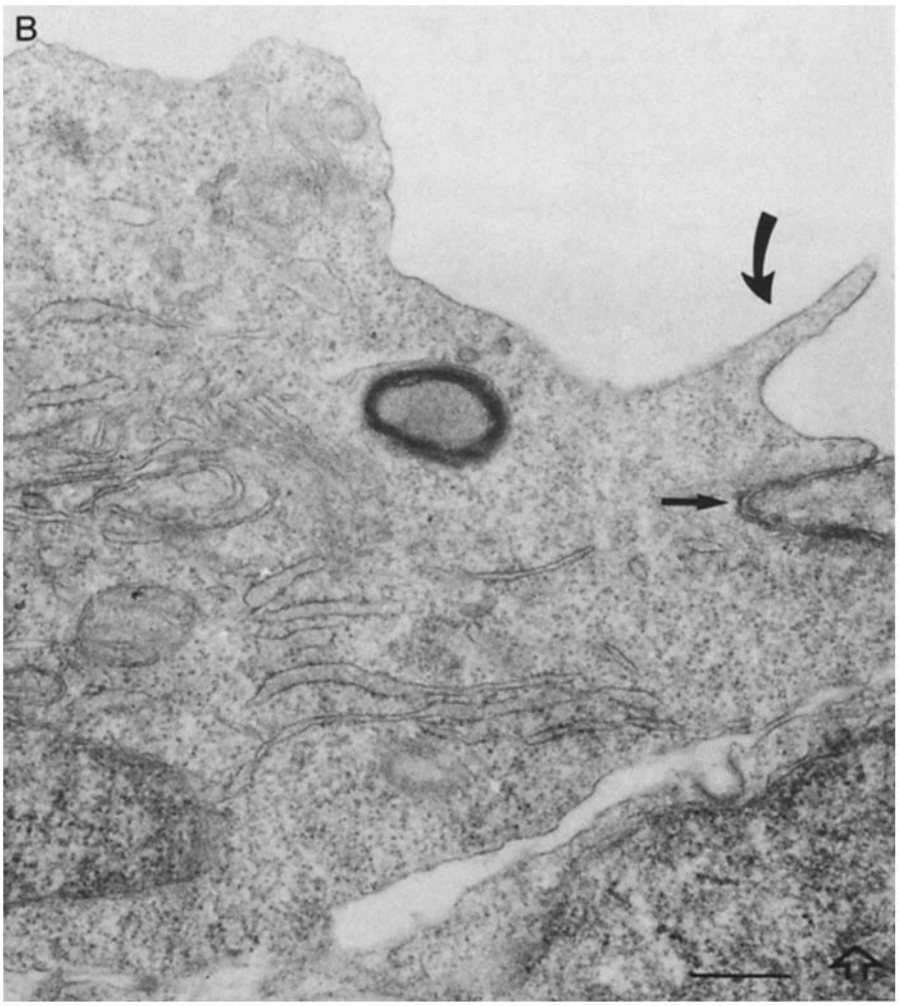

Figure 5. NCAM immunoreactivity on neuron and glia somata. (*A*) Neuron rising above a glial cell is heavily labeled with gold (*arrowheads*), while the glial cell has only a single gold particle on it (*small arrow*). (*B*) Nonneuronal phase-bright glial or ependymal cell has adhering membrane specialization between it and neighboring cell (*straight arrow*). Microvilli extensions (*curved arrow*) from these phase-bright nonneuronal cells are common and do not stain for NCAM. Hollow arrows point up from bottom of culture dish. E18 hypothalamus after 4 d in vitro. Bar, 0.43 μm.

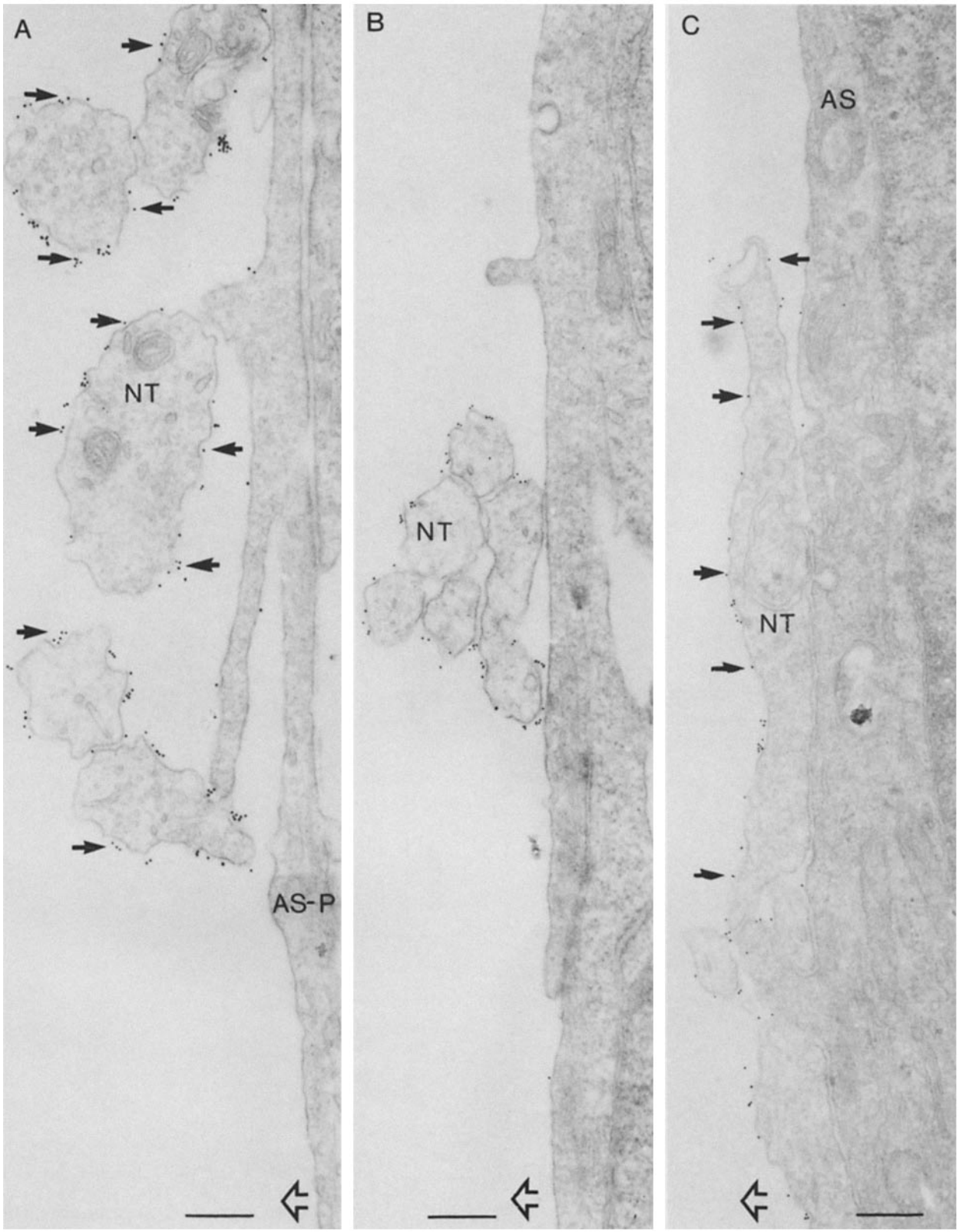

Figure 6. Immunogold labeling of NCAM on neurites. Neurites (*NT*) cut in cross section (*A* and *B*: bar, 0.23 μm) or parallel their long axis (*C*: bar, 0.24 μm). All are labeled with colloidal gold except for some regions of neurite–neurite contact which are probably inaccessible to the immunogold reagent. Hollow arrows point up from bottom of culture dish. Astrocytes (*AS*) and their processes (*AP*) are relatively unlabeled. E18 hypothalamus after 4 d in vitro.

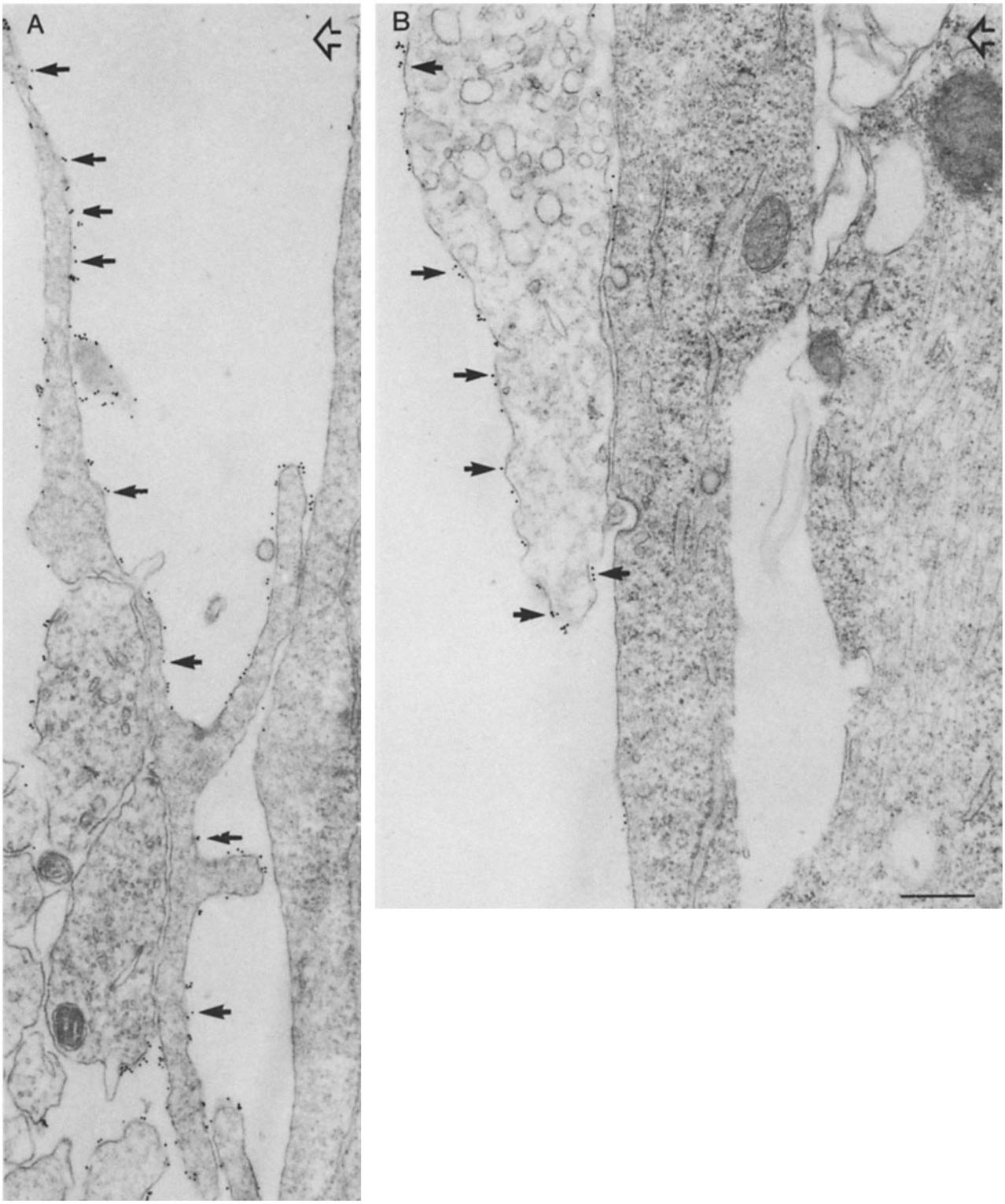

Figure 7. NCAM immunoreactivity on filopodia and growth cones. (*A*) Thin extensions from a neuronal process, possibly filopodia in a retraction phase, or after breaking free from an anchoring substrate. (*B*) A profile typical of section tangential to growing tip of axon, heavily labeled with colloidal gold. Large clear vesicles, typical of growth cones, are found in the process. Hollow arrows point up from bottom of culture dish. E18 hypothalamus after 4 d in vitro. Bar, 0.41 μm.

constant. If these results are representative of NCAM expression in vivo, they would suggest that a hypothetical NCAM-mediated guidance of a particular axon is more likely to reflect variation in the NCAM expression of cells that constitute the pathway rather than a heterogeneity within the growth cone. In addition, since a small increase in the density of NCAM can cause a substantial enhancement of adhesiveness (20), the significant variation in NCAM levels observed be-

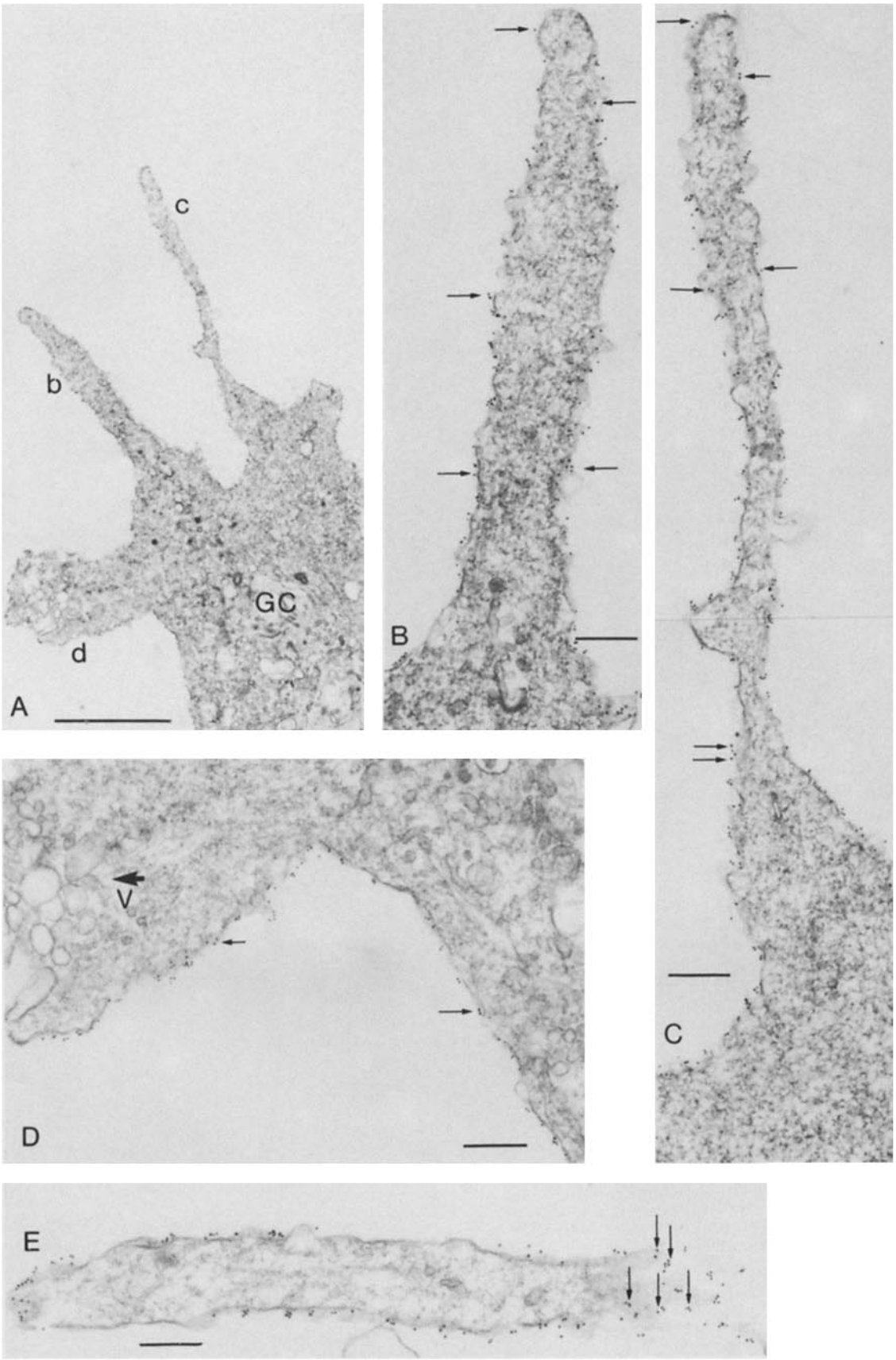

Figure 8. (*A*) Growth cone shown at low magnification. Bar, 2.1 μm. (*B* and *C*) Extension from growth cone indicated respectively by *b* and *c* in *A*. After staining with antiserum against NCAM, colloidal gold particles are found extending along the membrane from the base to the tip of these processes. (*D*) Typical of growth cones, large clear vesicles (*V*) can be found in *d*. Gold is found decorating both the base of the growth cone as well as more distal regions. Bar (*B–D*) 0.3 μm. (*E*) Filopodium distal to the growth cone is labeled with colloidal gold seen on a grazing section (*arrows*) of membrane at the distal end of the filopodium. Bar, 0.22 μm. Section parallel to bottom of culture dish. E16 hypothalamus after 4 d in vitro.

tween neurons in the present study might provide a basis for differential behavior of growing neurites.

In discussing our results, we have focused on NCAM. However, as indicated in the Introduction, many other molecules and parameters contribute to the overall process of axon guidance. Neurons taken from different regions of the CNS contain different densities of lectin receptors, and also contain different numbers of these receptors on different parts of growing neurites (32, 33). Monoclonal antibodies raised against neuronal membranes provide further evidence that certain molecules are only expressed on small numbers of neuronal surfaces in leech (57), grasshopper (12), and mammalian peripheral and central nervous systems (9, 10, 49). The possible roles of these molecules in cell recognition and axonal guidance have not been fully elucidated. Even with respect to NCAM, additional factors remain to be considered, namely that the molecule has several polypeptide forms and that the adhesive properties of NCAM are affected by natural variations in its content of polysialic acid (4, 20, 30).

The expression of NCAM on glial cells appears to be variable, ranging from a robust immunoreactivity on some glia in mouse and chicken tissues (23, 25, 45) and cultured rat astrocytes (29) to the sparse levels or absence of detectable NCAM found in the present studies of cultured rat cells, and on cultured chicken (15) glial-like flat cells and mouse astrocytes (18). These differences could reflect variations in the structure of NCAM (24, 30, 56), or in different experimental or cellular environmental conditions.

In summary, several converging lines of evidence presented in the Results demonstrate that the NCAM antigen is present on neuronal growth cones, including their lamellipodia and filopodia. These results are consistent with previous studies (40, 45), suggesting that guidance of axons can involve homophilic (NCAM–NCAM) interactions between growth cones and a second cellular surface that expresses NCAM.

We thank Mr. Peter Calabresi for help with some preliminary experiments and Ms. K. Szigeti and G. Collins for technical assistance.

Support was provided by National Institutes of Health Grants NS 16296, NS 10174, HD 18369, and the American Parkinson Disease Association.

Received for publication 9 September 1985, and in revised form 10 February 1986.

References

1. Bray, D. 1970. Surface movements during the growth of single explanted neurons. *Proc. Natl. Acad. Sci. USA.* 65:905–910.

2. Bray, D. 1979. Mechanical tension produced by nerve cells in tissue culture. *J. Cell. Sci.* 37:391–410.

3. Bunge, M. B. 1973. Fine structure of nerve fibers and growth cones of isolated sympathetic neurons in culture. *J. Cell Biol.* 56:713–735.

4. Cunningham, B. A., S. Hoffman, U. Rutishauser, J. J. Hemperly, and G. M. Edelman. 1983. Molecular topography of the neural cell adhesion molecule N-CAM: surface orientation and location of sialic acid-rich and binding regions. *Proc. Natl. Acad. Sci. USA.* 80:3116–3120.

5. DeMey, J., M. Moeremans, G. Geuens, R. Nuydens, and M. De-Brabander. 1981. High resolution light and electron microscopic localization of tubulin with the IGS (immuno gold staining) method. *Cell Biol. Int. Rep.* 5:889–899.

6. Denis-Donini, S., J. Glowinski, and A. Prochiantz. 1984. Glial heterogeneity might define the three-dimensional shape of neurons. *Nature (Lond.).* 307:641–643.

7. di Porzio, U., M.-C. Daguet, J. Glowinski, and A. Prochiantz. 1980. Effect of striatal cells on in vitro maturation of mesencephalic dopaminergic neurones grown in serum-free conditions. *Nature (Lond.).* 288:370–373.

8. di Porzio, U., and M. Estenoz. 1984. Positive control of target cerebellar cells on norepinephrine uptake in embryonic brain stem cultures in serum-free medium. *Dev. Brain. Res.* 16:147–157.

9. di Porzio, U., G. Rougon, J. Mazzetta, W. Kell, and J. Barker. 1985. Use of cell surface-directed monoclonal antibodies to isolate and study cultured neuronal subpopulations from the developing mouse CNS. *Soc. Neurosci. Abstr.* 11:978.

10. Dodd, J., D. Solter, and T. M. Jessell. 1984. Monoclonal antibodies against carbohydrate differentiation antigens identify subsets of primary sensory neurones. *Nature (Lond.).* 311:469–472.

11. Edelman, G. M., and C.-M. Chuong. 1982. Embryonic to adult conversion of neural cell adhesion molecules in normal and staggerer mice. *Proc. Natl. Acad. Sci. USA.* 79:7036–7040.

12. Goodman, C. S., M. J. Bastiani, C. Q. Doe, S. du Lac, S. L. Helfand, J. Y. Kuwada, and J. B. Thomas. 1984. Cell recognition during neuronal development. *Science (Wash. DC).* 225:1271–1279.

13. Goridis, C., H. Deagostini-Bazin, M. Hirn, M. R. Hirsch, G. Rougon, R. Sadoul, O. K. Langley, and G. Gombos. 1983. Neural surface antigens during nervous system development. *Cold Spring Harbor Symp. Quant. Biol.* 48:527–537.

14. Grumet, M., U. Rutishauser, and G. M. Edelman. 1982. Neural cell adhesion molecule is on embryonic muscle cells and mediates adhesion to nerve cells in vitro. *Nature (Lond.).* 295:693–695.

15. Grumet, M., U. Rutishauser, and G. M. Edelman. 1983. Neuron-glia adhesion is inhibited by antibodies to neural determinants. *Science (Wash. DC).* 222:60–62.

16. Hall, A. K., and U. Rutishauser. 1985. Phylogeny of a neural cell adhesion molecule. *Dev. Biol.* 110:39–46.

17. Harrison, R. G. 1910. Observations on the living developing nerve fiber. *Anat. Rec.* 1:116–118.

18. Hirn, M., M. Pierres, H. Deagostini-Bazin, M. Hirsch, and C. Goridis. 1981. Monoclonal antibody against cell surface glycoprotein of neurons. *Brain Res.* 214:433–439.

19. His, W. 1887. Die Entwicklung der ersten Nervenbahnen beim menschlichen Embryo: Uebersichtliche Darstellung. *Arch. Anat. Physiol. Leipzig. Anat. Abt.* 92:368–378.

20. Hoffman, S., and G. M. Edelman. 1983. Kinetics of homophilic binding by embryonic and adult forms of the neural cell adhesion molecule. *Proc. Natl. Acad. Sci. USA.* 80:5762–5766.

21. Horisberger, M., and J. Rosset. 1977. Colloidal gold, a useful marker for transmission and scanning electron microscopy. *J. Histochem. Cytochem.* 25:295–305.

22. Hsu, S., L. Raine, and H. Fanger. 1981. Use of avidin-biotin-peroxidase complex (ABC) in immunoperoxidase techniques: a comparison between ABC and unlabeled antibody (PAP) procedures. *J. Histochem. Cytochem.* 29:577–580.

23. Keilhauer, G., A. Faissner, and M. Schachner. 1985. Differential inhibition of neurone-neurone, neurone-astrocyte and astrocyte-astrocyte adhesion by L1, L2 and N-CAM antibodies. *Nature (Lond.).* 316:728–730.

24. Kruse, J., R. Mailhammer, H. Wernecke, A. Faissner, I. Sommer, C. Goridis, and M. Schachner. 1984. Neural cell adhesion molecule and myelin-associated glycoprotein share a common carbohydrate moiety recognized by monoclonal antibodies L2 and HNK-1. *Nature (Lond.).* 311:153–155.

25. Langley, O. K., M. S. Ghandour, G. Gombos, M. Hirn, and C. Goridis. 1982. Monoclonal antibodies as neural cell surface markers. *Neurochem. Res.* 7:349–362.

26. Letourneau, P. C. 1975. Cell-to-substratum adhesion and guidance of axonal elongation. *Dev. Biol.* 44:92–101.

27. Letourneau, P. C. 1982. Nerve fiber growth and its regulation by extrinsic factors. *In* Neuronal Development. C. Spitzer, editor. Plenum Publishing Company, New York. 213–254.

28. Levi-Montalcini, A. 1982. Developmental neurobiology and the natural history of nerve growth factor. *Annu. Rev. Neurosci.* 5:341–362.

29. Noble, M., M. Albrechtsen, C. Moller, J. Lyles, E. Bock, C. Goridis, M. Watanabe, and U. Rutishauser. 1985. Glial cells express N-CAM/D2-CAM-like polypeptides in vitro. *Nature (Lond.).* 316:725–728.

30. Nybroe, O., M. Albrechtsen, J. Dahlin, D. Linnemann, J. M. Lyles, C. J. Moller, and E. Bock. 1985. Biosynthesis of the neural cell adhesion molecule: characterization of polypeptide C. *J. Cell Biol.* 101:2310–2315.

31. Patel, N. B., and M.-M. Poo. 1984. Perturbation of the direction of neurite growth by pulsed and focal electric fields. *J. Neurosci.* 4:2939–2947.

32. Pfenninger, K. H., and M.-F. Maylie-Pfenninger. 1981. Lectin labeling of sprouting neurons. I. Regional distribution of surface glycoconjugates. *J. Cell Biol.* 89:536–546.

33. Pfenninger, K. H., and M.-F. Maylie-Pfenninger. 1981. Lectin labeling of sprouting neurons. II. Relative movement and appearance of glycoconjugates during plasmalemmal expansion. *J. Cell Biol.* 89:547–539.

34. Prochiantz, A., U. di Porzio, A. Kato, B. Berger, and J. Glowinski. 1979. In vitro maturation of mesencephalic dopaminergic neurons from mouse embryos is enhanced in presence of their striatal target cells. *Proc. Natl. Acad. Sci. USA.* 76:5387–5391.

35. Ramon y Cajal, S. 1890. Sur l'origine et les ramifications des fibres nerveuses de la moelle embryonaire. *Anat. Anz.* 5:609–631.

36. Ramon y Cajal, S. 1908. Nouvelles observations sur l'evolution des neuroblasts avec quelques remarques sur l'hypothese neurogenetique de Hensen-Held. *Anat. Anz.* 23:1–25;65–87.

37. Rougon, G., M. R. Hirsch, M. Hirn, J. L. Guenet, and C. Goridis. 1983. Monoclonal antibody to neural cell surface protein: identification of a glycoprotein family of restricted cellular localization. *Neuroscience.* 10:511–522.

38. Rutishauser, U. 1984. Developmental biology of a neural cell adhesion molecule. *Nature (Lond.).* 310:549–554.

39. Rutishauser, U. 1985. Influences of the neural cell adhesion molecule on axon growth and guidance. *J. Neurosci. Res.* 13:123–131.

40. Rutishauser, U., W. E. Gall, and G. M. Edelman. 1978. Adhesion among neural cells of the chick embryo. IV. Role of the cell surface molecule CAM in the formation of neurite bundles in cultures of spinal ganglia. *J. Cell Biol.* 79:382–393.

41. Rutishauser, U., M. Grumet, and G. M. Edelman. 1983. N-CAM mediates initial interactions between spinal cord neurons and muscle cells in culture. *J. Cell Biol.* 97:145–152.

42. Rutishauser, U., S. Hoffman, and G. M. Edelman. 1982. Binding properties of a cell adhesion molecule from neural tissue. *Proc. Natl. Acad. Sci. USA.* 79:685–689.

43. Rutishauser, U., J. P. Thiery, R. Brackenbury, and G. M. Edelman. 1978. Adhesion among neural cells of the chick embryo. III. Relationship of the surface molecule CAM to cell adhesion and the development of histotypic patterns. *J. Cell Biol.* 79:371–381.

44. Sidman, R. L., and N. K. Wessels. 1975. Control of direction of growth during the elongation of neurites. *Exp. Neurol.* 48:237–251.

45. Silver, J., and U. Rutishauser. 1984. Guidance of optic axons by a preformed adhesive pathway on neuroepithelial endfeet. *Dev. Biol.* 106:485–499.

46. Singer, M., N. Nordlander, and N. Egar. 1979. Axonal guidance during embryogenesis and regeneration in the spinal cord of the newt. The blueprint hypothesis of neuronal pathway patterning. *J. Comp. Neurol.* 185:1–22.

47. Sperry, R. 1963. Chemoaffinity in the orderly growth of nerve fiber patterns and connections. *Proc. Natl. Acad. Sci. USA.* 50:703–710.

48. Thanos, S., F. Bonhoeffer, and U. Rutishauser. 1984. Fiber-fiber interactions and tectal cues influence the development of the chick retinotectal projection. *Proc. Natl. Acad. Sci. USA.* 81:1906–1910.

49. Trisler, G. D., M. D. Schneider, and M. Nirenberg. 1981. A topographic gradient of molecules in retina can be used to identify neuron position. *Proc. Natl. Acad. Sci. USA.* 78:2145–2150.

50. van den Pol, A. N. 1984. Colloidal gold and biotin-avidin conjugates as ultrastructural markers for neural antigens. *Q. J. Exp. Physiol. Cogn. Med. Sci.* 69:1–33.

51. van den Pol, A. N. 1985. Dual ultrastructural localization of two neurotransmitter-related antigens: colloidal gold labeled neurophysin immunoreactive supraoptic neurons receive peroxidase labeled glutamate decarboxylase or gold labeled GABA immunoreactive synapses. *J. Neurosci.* 5:2940–2954.

52. van den Pol, A. N., U. diPorzio, and U. Rutishauser. 1985. Neural cell adhesion molecule (NCAM) localization on plasmalemmal surfaces of primary culture central nervous system. *J. Cell Biol.* 101 (5, Pt. 2):123*a*. (Abstr.)

53. van den Pol, A. N., R. S. Herbst, and J. F. Powell. 1984. Tyrosine hydroxylase-immunoreactive neurons of the hypothalamus: a light and electron microscopic study. *Neuroscience.* 13:1117–1156.

54. van den Pol, A. N., and K. Tsujimoto. 1985. Neurotransmitters of the hypothalamic suprachiasmatic nucleus: immunocytochemical analysis of 25 neuronal antigens. *Neuroscience.* 15:1049–1086.

55. Weiss, P. 1941. Nerve patterns: the mechanics of nerve growth. *3rd Growth Symp.* 5:163–203.

56. Williams, R. K., C. Goridis, and R. Akeson. 1985. Individual neural cell types express immunologically distinct N-CAM forms. *J. Cell Biol.* 101:36–42.

57. Zipser, B., and R. McKay. 1981. Monoclonal antibodies distinguish identifiable neurons in the leech. *Nature (Lond.).* 289:549–554.